**Supplementary Material**

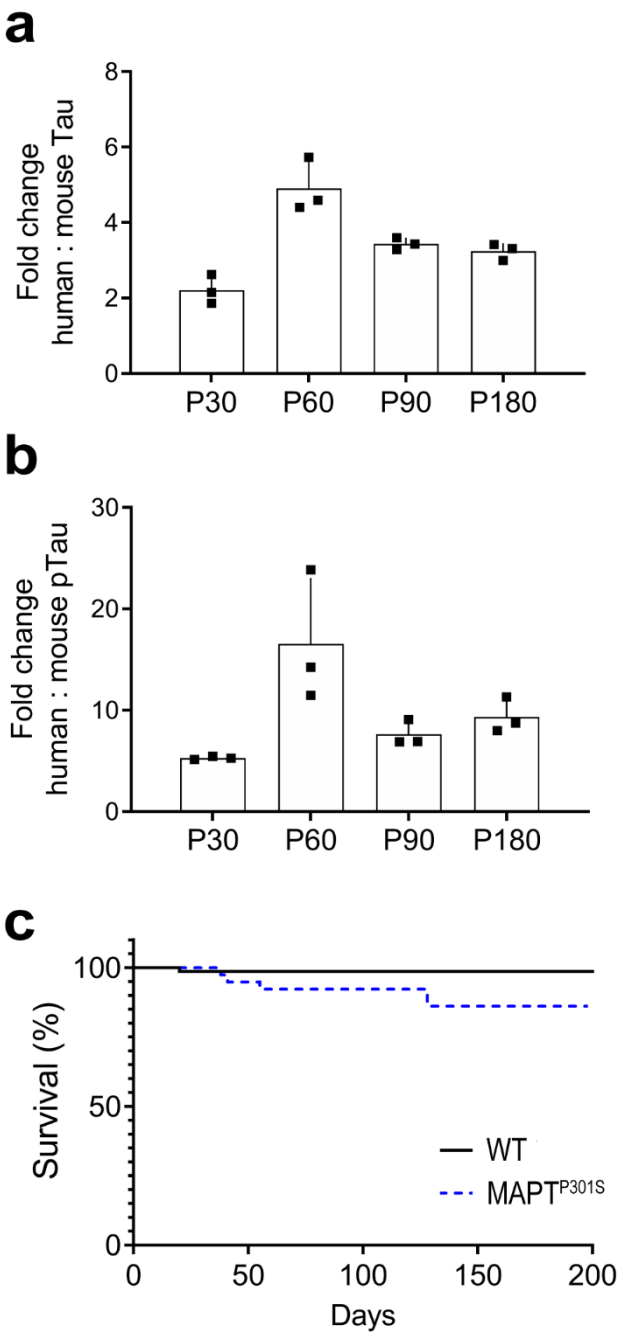


**Figure S1. Human tau protein expression is 2 to 5-fold higher than endogenous mouse tau in *MAPT*$^{P301S}$ mice**

**a**) Fold change between human tau and mouse tau in *MAPT*$^{P301S}$ mice at P30, P60, P90 and P180. **b**) Fold change between human phosphorylated tau and mouse phosphorylated tau in *MAPT*$^{P301S}$ mice at P30, P60, P90 and P180. Results are presented as mean ± SD, n = 3 mice per genotype. **c**) 86% of *MAPT*$^{P301S}$ mice (n = 39) survived to P200 against 98% of WT mice (n = 73). Survival curves comparison: Log-Rank (Mantel-Cox), p = 0.0390.

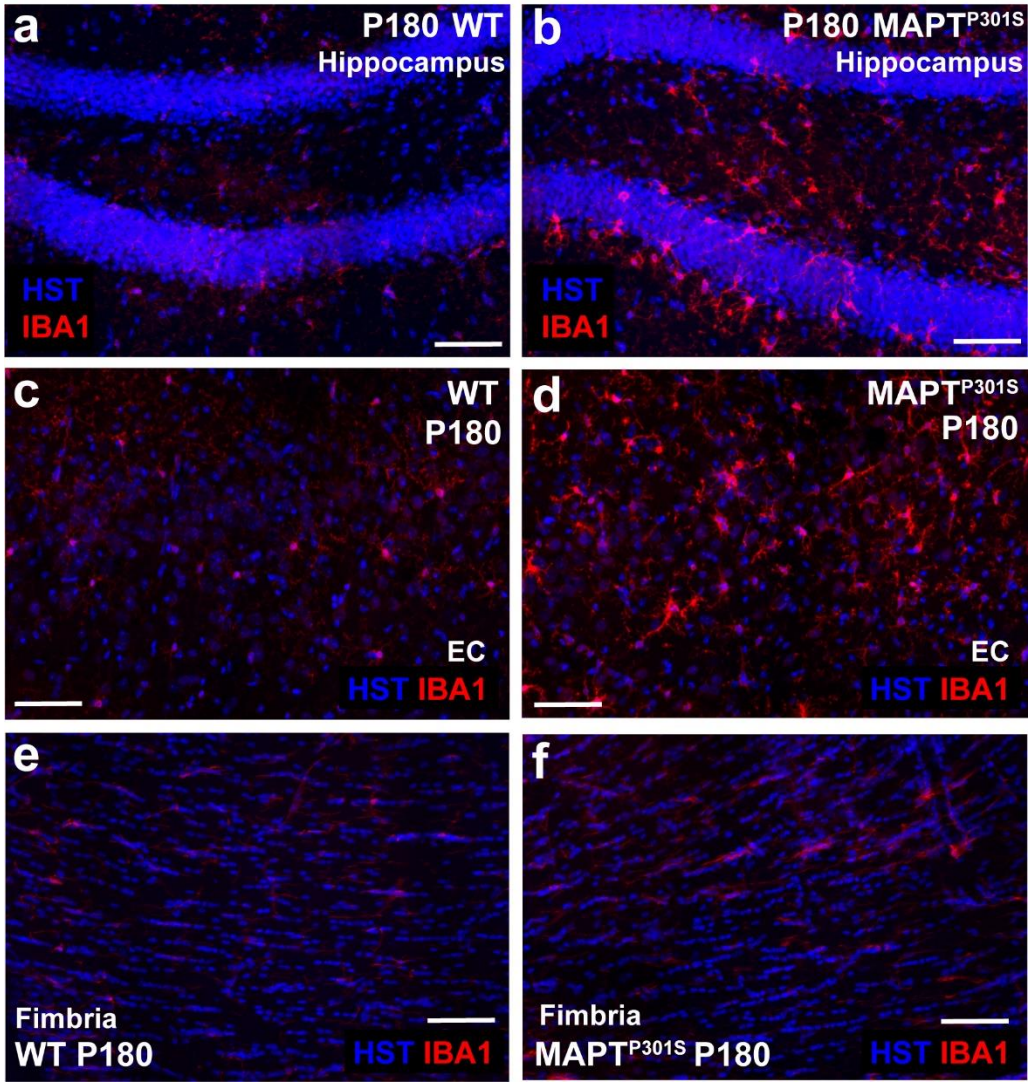


**Figure S2. Reactive microglia are visible in *MAPT*$^{P301S}$ mice at P180**

**a-f**) Representative confocal images of Iba1 (red) and Hoechst 33342 (blue) in the hippocampus (**a-b**), entorhinal cortex (EC; **c-d**) and fimbria (**e-f**) of wildtype (**a, c, e**) and *MAPT*$^{P301S}$ (**b, d, f**) mice at P180. Scale bars represent 60µm.

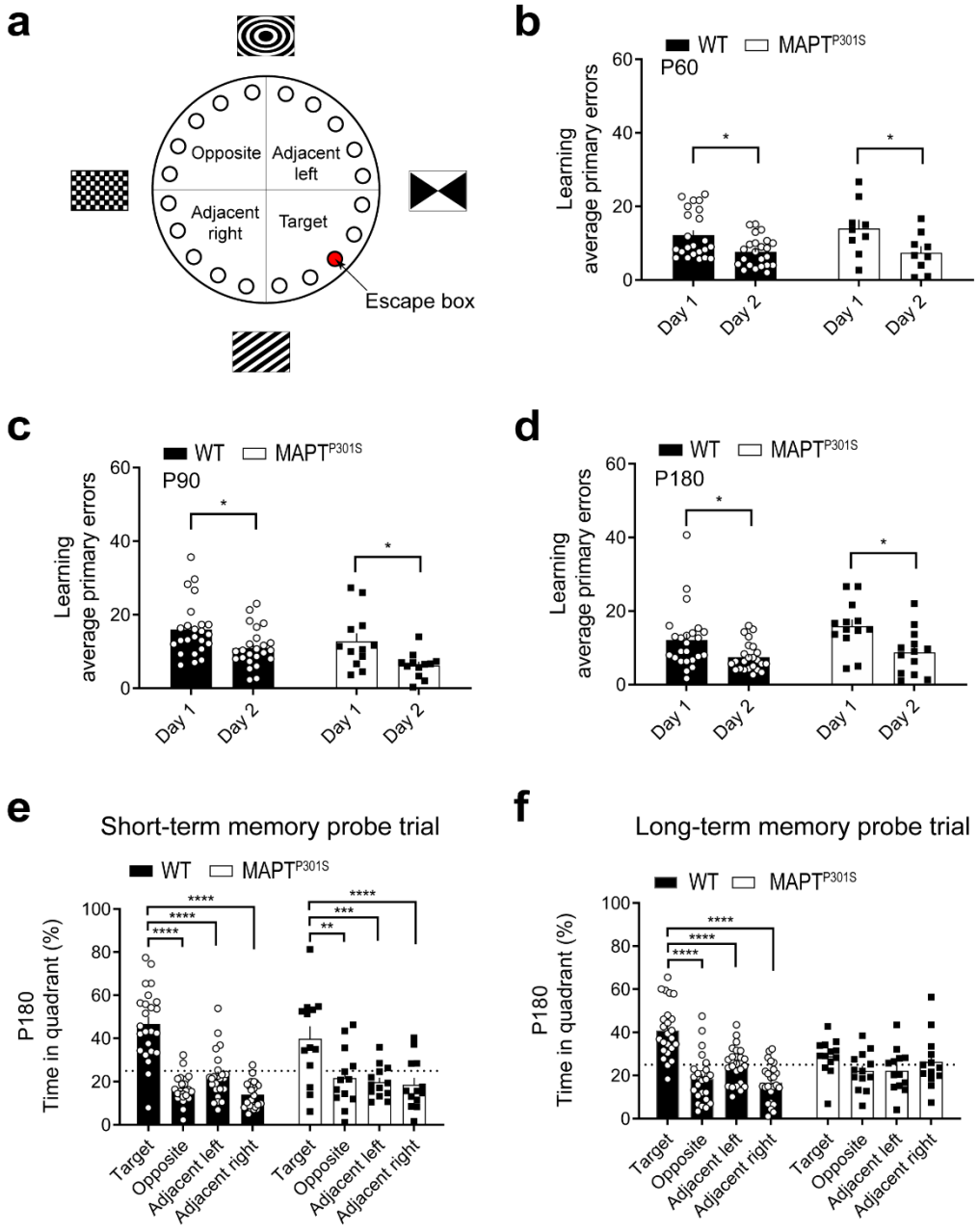


**Figure S3. Learning and memory performance in the Barnes maze**

**a**) Schematic diagram of the Barnes maze depicting the location of the escape box (red) relative to the spatial cues surrounding the maze and quadrant divisions. **b**) Quantification of the average number primary errors committed by P60 WT (open circles, black bars) and *MAPT*$^{P301S}$ (black squares, open bars) mice during the first and second day of learning [two-way ANOVA, genotype: F (1, 60) = 0.24, p = 0.6233; learning day: F (1, 60) = 12.46, p = 0.0008; interaction: F (1, 60) = 0.39, p = 0.5307]. **c**) Quantification of the average number primary errors committed by P90 WT and *MAPT*$^{P301S}$ mice during the first and second day of learning [two-way ANOVA, genotype: F (1, 68) = 6.30, p = 0.0144; learning day: F (1, 68) = 13.37, p = 0.0005; interaction: F (1, 68) = 0.25, p = 0.6166]. **d**) Quantification of the average number primary errors committed by P180 WT and *MAPT*$^{P301S}$ mice during the first and second day of learning [two-way ANOVA, genotype: F (1, 70) = 2.569, p = 0.1135; learning day: F (1, 70) = 13.91, p = 0.0004; interaction: F (1, 70) = 0.5959, p = 0.4428]. **e**) Quantification of the time spent

by P180 WT and *MAPT*$^{P301S}$ mice in each quadrant of the maze during the short-term memory probe phase [two-way ANOVA, genotype: F (1, 140) = 6.558e-006, p = 0.9980; maze quadrant: F (3, 140) = 35.37, p < 0.0001; interaction: F (3, 140) = 1.959, p = 0.1230]. **f**) Quantification of the time spent by P180 WT and *MAPT*$^{P301S}$ mice in each quadrant of the maze during the long-term memory probe phase [two-way ANOVA, genotype: F (1, 140) = 0.033, p = 0.8550; maze quadrant: F (3, 140) = 14.14, p < 0.0001; interaction: F (3, 140) = 6.737, p = 0.0003]. Data are presented as mean ± SEM, n= 13-24 mice per group.

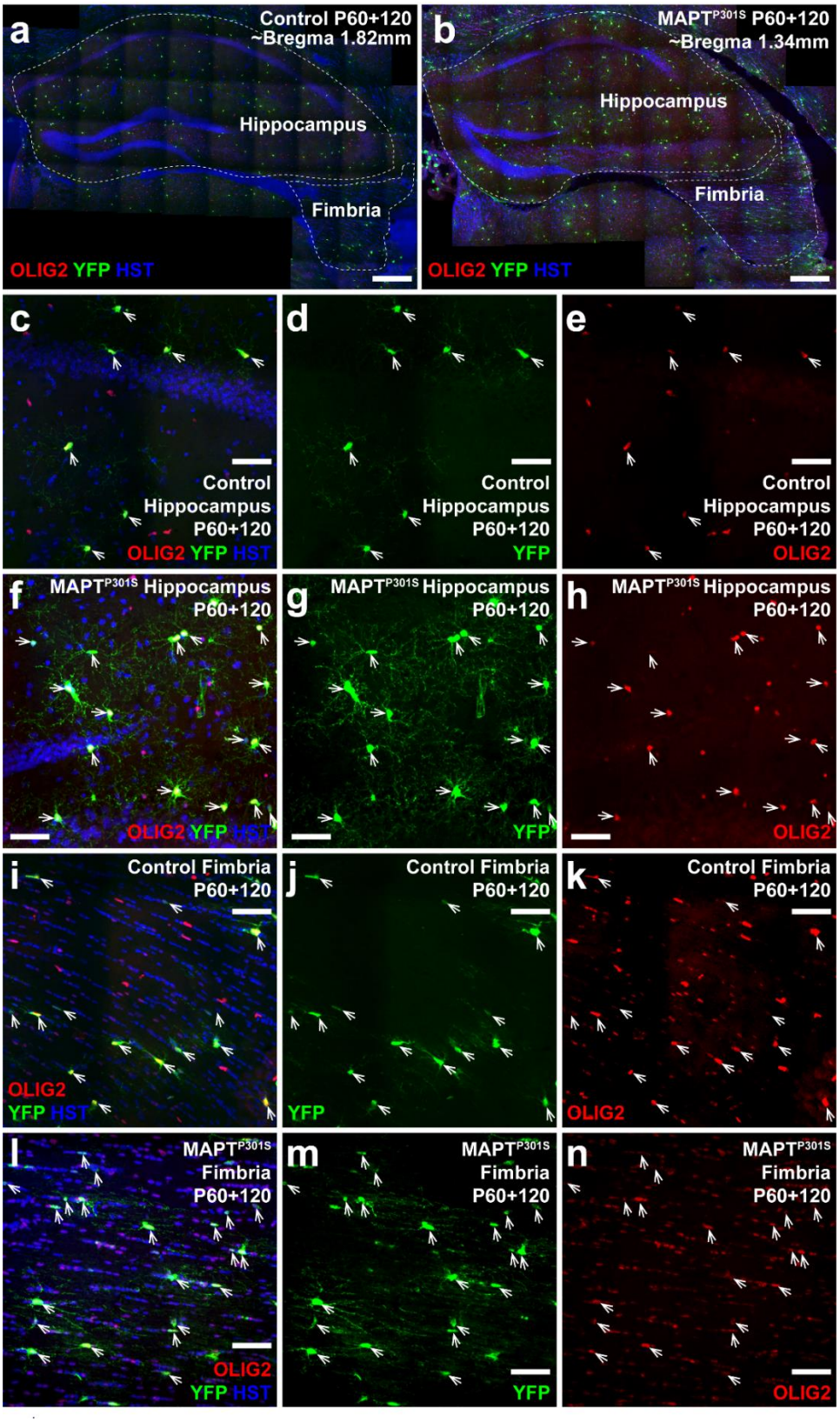


**Figure S4. Essentially all YFP$^{+}$ cells express OLIG2 in P60+120 control and *MAPT$^{P301S}$* mice**

**a-b**) Low magnification confocal image showing the hippocampus and fimbria in coronal brain cryosections from P60+120 control and *MAPT$^{P301S}$* transgenic mice stained to detect YFP (green), OLIG2 (red) and Hoechst 33342

(blue). **c-e**) Confocal image of the hippocampus in coronal brain cryosections from P60+120 control mice stained to detect YFP (green), OLIG2 (red) and Hoechst 33342 (blue). **f-h**) Confocal image of the hippocampus in coronal brain cryosections from P60+120 $MAPT^{P301S}$ transgenic mice stained to detect YFP (green), OLIG2 (red) and Hoechst 33342 (blue). **i-k**) Confocal image of the fimbria in coronal brain cryosections from P60+120 control mice stained to detect YFP (green), OLIG2 (red) and Hoechst 33342 (blue). **l-n**) Confocal image of the fimbria in coronal brain cryosections from P60+120 *$MAPT^{P301S}$* mice stained to detect YFP (green), OLIG2 (red) and Hoechst 33342 (blue). White arrows indicate $YFP^+$ $OLIG2^+$ cells. Scale bar represents 280 µm (a-b), 50 µm (c-h), or 25 µm (i-k).

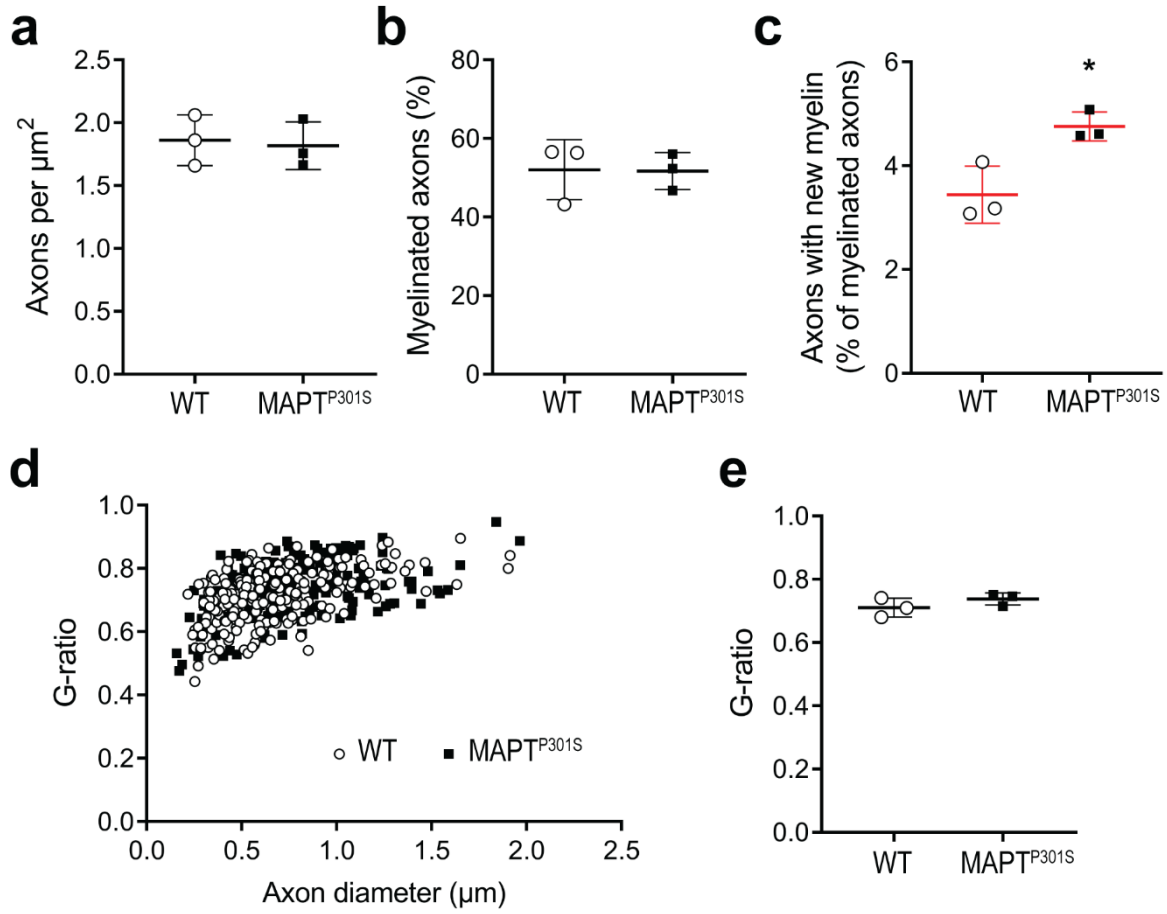


**Figure S5. The proportion of newly myelinated axons is increased in the fimbria of P180 *MAPT*$^{P301S}$ mice**

**a)** Quantification of axon density (axons / µm$^2$) in the fimbria of P180 WT (open circles) and *MAPT*$^{P301S}$ (black squares) mice (two-tailed t-test, t = 0.2750, df = 4, p = 0.7970). **d**) Quantification of the proportion of myelinated axons in the CA1 of WT and *MAPT*$^{P301S}$ mice at P180 (two-tailed t-test, t = 0.0635, df = 4 p = 0.9524). **e**) Quantification of the proportion of myelinated axons ensheathed by immature (new) myelin (two-tailed t-test, t = 3.695, df = 4, p = 0.0209). **f**) Graphical representation of the g-ratio distribution based on axon diameter (Simple linear regression analysis, slope F (1, 524) = 1.735, p = 0.1884, Y intercept F (1, 525) = 5.422, p = 0.0203 n = 64 - 109 myelinated axons per mouse). g) Quantification of average g-ratio per animal in WT and *MAPT*$^{P301S}$ mice at P180 (two-tailed t-test, t = 1.324, df = 4, p = 0.2562). n = 3 animals per genotype.